



# A novel approach to quantify the assistive torque profiles generated by passive back-support exoskeletons

Saman Madinei<sup>a</sup>, Sunwook Kim<sup>a</sup>, Jang-Ho Park<sup>b</sup>, Divya Srinivasan<sup>b</sup>, Maury A. Nussbaum<sup>a,\*</sup>

<sup>a</sup> Department of Industrial and Systems Engineering, Virginia Tech, Blacksburg, VA 24061, USA

<sup>b</sup> Department of Industrial Engineering, Clemson University, Clemson, SC 29634, USA

## ARTICLE INFO

**Keywords:**  
Biomechanics  
Musculoskeletal modeling  
Stiffness  
Wearable technology

## ABSTRACT

Industrial exoskeletons are a promising ergonomic intervention to reduce the risk of work-related musculoskeletal disorders by providing external physical support to workers. Passive exoskeletons, having no power supplies, are of particular interest given their predominance in the commercial market. Understanding the mechanical behavior of the torque generation mechanisms embedded in passive exoskeletons is, however, essential to determine the efficacy of these devices in reducing physical loads (e.g., in manual material handling tasks). We introduce a novel approach using a computerized dynamometer to quantify the assistive torque profiles of two passive back-support exoskeletons (BSEs) at different support settings and in both static and dynamic conditions. The feasibility of this approach was examined using both human subjects and a mannequin. Clear differences in assistive torque magnitudes were evident between the two BSEs, and both devices generated more assistive torques during trunk/hip flexion than extension. Assistive torques obtained from human subjects were often within similar ranges as those from the mannequin, though values were more comparable over a narrow range of flexion/extension angles due to practical limitations with the dynamometer and human subjects. Characterizing exoskeleton assistive torque profiles can help in better understanding how to select a torque profile for given task requirements and user anthropometry, and aid in predicting the potential impacts of exoskeleton use by incorporating measured torque profiles in a musculoskeletal modeling system. Future work is recommended to assess this approach for other occupational exoskeletons.

## 1. Introduction

Occupational exoskeletons act to support/augment the physical capacity of a worker and thus have the potential to reduce physical demands and prevent work-related musculoskeletal disorders. Most commercially-available occupational exoskeletons are currently passive systems, which include compliant elements (e.g., springs or other elastic materials) to provide external torques about a joint of interest (e.g., back or shoulder). These external torques are generated as a function of the included angles between proximal and distal segments comprising the joint of interest. Compared to active/powered systems, passive exoskeletons are technologically more mature, and have been considered for a range of applications, including automotive manufacturing (Hensel & Keil, 2019; Ferreira et al., 2020; Kim et al., 2021), agriculture (Upasani et al., 2019; Thamsuwan et al., 2020), and construction (Kim et al., 2019; Moore et al., 2021). To promote the safe adoption and use of an exoskeleton, though, it is critical to determine the effects of using an

exoskeleton in diverse task scenarios. Indeed, numerous lab- and field-based studies have quantified the biomechanical effects of different exoskeletons on the user (e.g., Kim et al., 2018; Alabdulkarim & Nussbaum, 2019; Baltrusch et al., 2019; Koopman et al., 2019; Alemi et al., 2020; Koopman et al., 2020; Madinei et al., 2020; Kim et al., 2021). Given the resource-intensive nature of lab or field testing, however, and the increasing availability of different exoskeleton designs, an effective approach is needed to simulate or predict the impacts of exoskeleton use for potential occupational applications (Nussbaum et al., 2019).

Musculoskeletal modeling software could facilitate assessing exoskeleton use under various work scenarios. In fact, there are several reports of the impacts of exoskeleton use or different exoskeleton designs (e.g., support torque profiles) in which estimated muscle activities and joint forces/torques were derived using the AnyBody Modeling System (Agarwal et al., 2016; Jensen et al., 2018; Fritzsche et al., 2021) or OpenSim (de Kruif et al., 2017; Khamar et al., 2019; Zhou & Chen, 2021). When simulating human-exoskeleton interactions, however,

\* Corresponding author at: Department of Industrial and Systems Engineering, Virginia Tech, 250 Durham Hall (0118), Blacksburg, VA 24061, USA.  
E-mail address: [nussbaum@vt.edu](mailto:nussbaum@vt.edu) (M.A. Nussbaum).

mechanical aspects of an exoskeleton need to be defined in the modeling software environment. These aspects include component inertial properties, available degrees-of-freedom, and supportive torque profiles (i.e., torque–angle relationships). The latter is of particular importance, since exoskeletons have distinct torque-generating mechanisms. Exoskeleton manufacturers, though, typically treat these torque profiles as proprietary, likely because the profiles can substantially affect the effectiveness of an exoskeleton and a user's perception regarding exoskeleton use and its effectiveness. Furthermore, even if the manufacturers provide some baseline profiles for their device, systematic measurement of assistive torque profiles might be still needed, since some torque generation mechanisms may not be purely elastic, instead exhibiting viscoelastic behaviors (e.g., speed dependency and hysteresis).

Though some exoskeleton torque profiles have been reported using simulated data (Bartel & Davy, 2006; Hyun et al., 2019), there are only few reports of results using direct measures. Koopman et al. (2019; 2020) measured the torque profile of a particular back-support exoskeleton (BSE; Laevo™ V2.4, Delft, Netherlands). They placed a force transducer under the chest pad of the exoskeleton, likely because this pad is coupled with an external torque generator about each hip, and monitored the BSE kinematics (i.e., hip flexion/extension angle) using three markers. They reported no effect of flexion/extension speed on torque profiles, but that there was hysteresis present (i.e., supportive torques were larger during trunk flexion than extension). This approach is seemingly straightforward and easy to implement, but it permits only a limited control over exoskeleton angular velocity since a participant needs to voluntarily flex/extend the trunk. Further, placing a force transducer under the chest pad of a BSE could present a practical challenge depending on the design of the pad (e.g., having a large surface area), or if the torque-generating mechanism at the hip is structurally connected to the backside of a user's trunk.

Thus, we describe here an alternative approach to quantify torque profile(s) of an exoskeleton. We specifically implemented this approach on two different BSEs with distinct support settings, yet a similar approach may be used to quantify the torque profiles generated by passive arm-support exoskeletons. This approach uses a computerized isokinetic dynamometer, which permits accurate control of limb flexion/extension angles and angular velocities. We implemented this approach using both human subjects and a mannequin, to determine whether both might be feasible.

## 2. Methods

### 2.1. Back-support exoskeletons

We used the BackX™ Model AC and Laevo™ V2.5, which both incorporate passive torque-generating mechanisms about the hip that are intended to augment the trunk extensor muscles, yet which also have distinct design features. BackX™ support settings can be adjusted, four combinations of support, consisting of two *modes* (instant vs standard) and two *support levels* (low vs high). The instant mode provides assistive torque immediately after the wearer bends forward, while in the standard mode supportive torque is provided when trunk flexion reaches ~35°. In contrast, the Laevo™ allows for adjusting an “angle button” (0–35°) to alter support to a comfortable angle. According to the manufacturers' user manuals, these ranges of support levels are offered to allow flexibility for the users to balance the work demand and external support required (suitx.com, laevo-exoskeleton.com). The BackX™ was tested at low and high support levels in the instant mode, and the Laevo™ was tested at low (35°) and high (0°) angle buttons; these settings are subsequently referred to as BSE<sub>LOW</sub> and BSE<sub>HIGH</sub>, respectively. To isolate the torque profile mechanisms, an additional condition was included for both BSEs in which supportive torques were turned off (i.e., BSE<sub>OFF</sub>).

### 2.2. Experimental design and procedures

Torque profiles (i.e., torque vs angle/speed relationship) were measured using both the isometric and continuous passive motion (CPM) modes of a computerized isokinetic dynamometer (HUMAC NORM, CSMi, Stoughton, MA, USA). The former was used to obtain torque profiles under static conditions (i.e., constant joint angle) and the latter to obtain torque profiles during motion (i.e., flexing/extending the joint of interest). For a given BSE, separate torque profiles were measured in each of three supportive torque settings (i.e., BSE<sub>OFF</sub>, BSE<sub>LOW</sub>, and BSE<sub>HIGH</sub>) in both static and dynamic conditions. These torque profiles were obtained using both an articulated mannequin (MZ-HM01, RoxyDisplay, East Brunswick, NJ, USA) and human subjects. To derive the offset torque data, the torque profile of the mannequin was measured without “wearing” the BSEs (i.e., NO BSE). The mannequin had a hinge joint at the hip allowing for pure hip flexion/extension. Since the mannequin lacked soft tissues and had a body shape not representative of actual populations, testing using human subjects may produce more realistic motions of a BSE. However, human subjects testing would present other confounding factors due to potential voluntary or reflexive muscle activation during dynamic conditions.

#### 2.2.1. Use of the mannequin

To measure torque profiles, the mannequin was fitted with a BSE, then positioned and secured on the dynamometer bed such that the rotational center of the BSE torque generation mechanism (i.e., left hip joint center of the mannequin) was aligned to the rotational center of the dynamometer motor. Then, the left thigh of the mannequin was connected to the hip adapter of the dynamometer (Fig. 1). For the static condition, the isometric mode was configured to passively move the left thigh of the mannequin to 13 different hip joint angles (0, 10, 20, ..., 120°), then each angle was maintained for 10 s. For the dynamic conditions, the CPM mode was configured to operate over a range from 0° (neutral hip angle) to 120° (hip flexion) at five different angular speeds (20, 40, 60, 80, and 100°/sec.) that were intended to capture typical occupational task demands (e.g., Marras et al., 1993; Lavender et al., 2012). At each speed, the left thigh of the mannequin was driven passively and isokinetically over the set angular range 14 times, mimicking repetitive hip flexion and extension. In both static and dynamic conditions, dynamometer torques and angles were recorded at 100 Hz.

#### 2.2.2. Use of human subjects

Two male participants with respective mean (SD) age, height, and mass of 26.5 (3.5) yrs, 182.0 (5.7) cm, and 70.0 (7.1) kg completed testing. The research procedures were approved by the Institutional Review Board at Virginia Tech, and informed consent was obtained from the participants prior to any data collection. Participants were fitted with a BSE and asked to stand in the trunk modular component (TMC) of

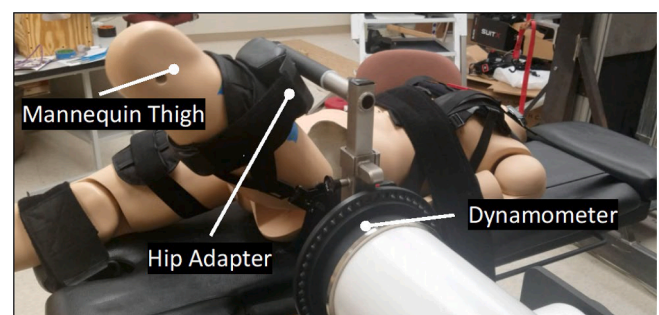


Fig. 1. Illustration of the experimental setup using a mannequin lying supine on the bed of a dynamometer. The mannequin is “wearing” the BackX™, and the left “thigh” was positioned or moved using a hip adapter connected to the dynamometer.

the HUMAC NORM. The TMC foot plate on which participants stood was then adjusted vertically so that the rotational center of the BSE torque-generating mechanism was aligned to the rotational center of the TMC, and participants were secured to the TMC following the manufacturer's recommendations (Fig. 2). For the static condition, as when the mannequin was used, the isometric mode was configured to passively move the trunk of participants to each of 10 trunk flexion angles (0, 10, 20, ..., 90°), and isometric torques were measured for 10 s. During dynamic trials, the CPM mode was configured to operate over a range of 0° (standing upright) to 90° (trunk flexion) at the same five joint speeds as when the mannequin was used. Note that we used 90° instead of 120° as the maximum trunk flexion angle due to a mechanical limitation of the TMC and to accommodate participant range-of-motion and comfort.

For each angular speed, participants first completed 10 training trials, during which they were repeatedly asked to limit abdominal muscle activity to minimize confounding effects on measured torques. This training was accomplished using real-time visual feedback of bilateral rectus abdominus (RA) activity, via normalized surface electromyography (EMG). Trunk extensors were not monitored as they did not show any reflexive responses to flexion/extension. Electrode placements were performed based on previous guidelines (Criswell, 2010). Participants completed initial maximum voluntary isometric contractions (MVICs), using the dynamometer to isolate the pelvis and lower extremities. Participants were secured to the trunk adapter with their

trunk flexed 20° and performed active trunk flexion (Marras & Mirka, 1993). MVICs were replicated twice, during which non-threatening verbal encouragement was provided. Raw EMG signals were recorded at 2 kHz using a telemetered system (TeleMyo Desktop DTS, Noraxon, AZ, USA), and rest breaks of 30 s or longer were provided between MVICs. A rest break of 1 min or longer was provided after the training trials. EMG signals were band-pass filtered (20–450 Hz, 4th-order Butterworth, bidirectional) and subsequently low-pass filtered (3 Hz cut-off, 4th-order Butterworth, bidirectional) to create linear envelopes. During dynamic trials, the trunk of participants was driven passively and isokinetically over the set range-of-motion 14 times. Processed EMG signals during the dynamic trials were normalized (nEMG) to maximum values collected during MVICs. nEMGs were displayed during the noted trials via a monitor at roughly the participant's waist level, and participants were asked to maintain their nEMG values below 10 % MVIC.

### 2.3. Data reduction and outcome measures

Raw torque data were low-pass filtered (2nd-order, bidirectional Butterworth filter, cut-off frequency = 9 Hz). Raw torque and angle data were resampled at 100 points per angle (e.g., 120° x 100 = 12,000 data points for the mannequin) for subsequent analysis. These data were then separated into flexion and extension phases, and mean values were obtained across the 14 trials. Dynamic torques reported hereafter are for the low angular speed only (20°/sec), since at higher speeds there were more substantial effects of dynamometer acceleration/deceleration (see Results). We considered two approaches to derive the exoskeleton-generated net torque profiles: 1) subtracting angle-specific raw torques in the BSE<sub>OFF</sub> condition from each respective support condition (BSE<sub>HIGH</sub> and BSE<sub>LOW</sub>), and 2) subtracting angle-specific raw torques in the NO BSE condition from each respective support conditions (BSE<sub>HIGH</sub> and BSE<sub>LOW</sub>). For brevity, results presented hereafter are focused on the former. However, additional data on the offset raw torque profiles for the NO BSE condition are reported in the Appendix (Fig. A3). Assistive torque profiles are reported unilaterally (per torque-generating mechanism). Peak (95th percentile) nEMG values for the bilateral RA were obtained to characterize abdominal muscle activity.

## 3. Results

No substantial effects of speed were apparent for the assistive raw torques of either BSE during the flexion and extension phases, and the dynamic mannequin trials were qualitatively highly repeatable over the 14 replications (Fig. A1). Different raw torque profiles were recorded at the beginning and ending phases of movement, likely due to the angular acceleration/deceleration of the hip adapter. Both BSEs, though, generated more assistive torque during flexion than extension (Fig. 3). The maximum net torques offered by BackX™ were respectively 24.8, 19.2, and 17.9 Nm for the flexion, extension, and static conditions at high support, and 14.7, 11.3, and 11.3 Nm at low support. The respective values for the Laevo™ were 9.7, 6.4, and 8.5 Nm at high support, and 7.9, 6.4, and 5.9 Nm at the low support condition. (Recall that these values are torque outputs per unilateral mechanism.).

Assistive torques obtained from the human subjects were overall within similar ranges to those from the mannequin, with differences at each joint angle that were ~0–10 Nm depending on the specific BSE, joint angle, and support condition (Figs. 4 and 5). Further, peak RA activity was relatively low overall (<~8 %MVIC) and remained consistent when using either BSE at the different flexion/extension speeds (Table A1).

## 4. Discussion

We developed an approach to measure the assistive torque profiles of a BSE using a computerized dynamometer and used this approach to characterize torque profiles of two BSEs in different support settings

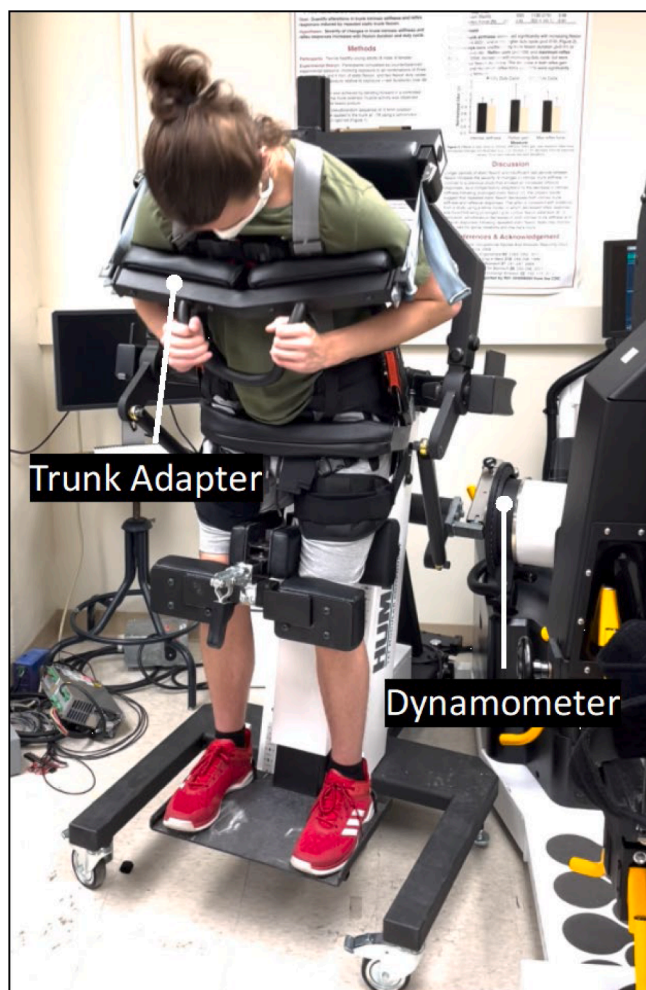
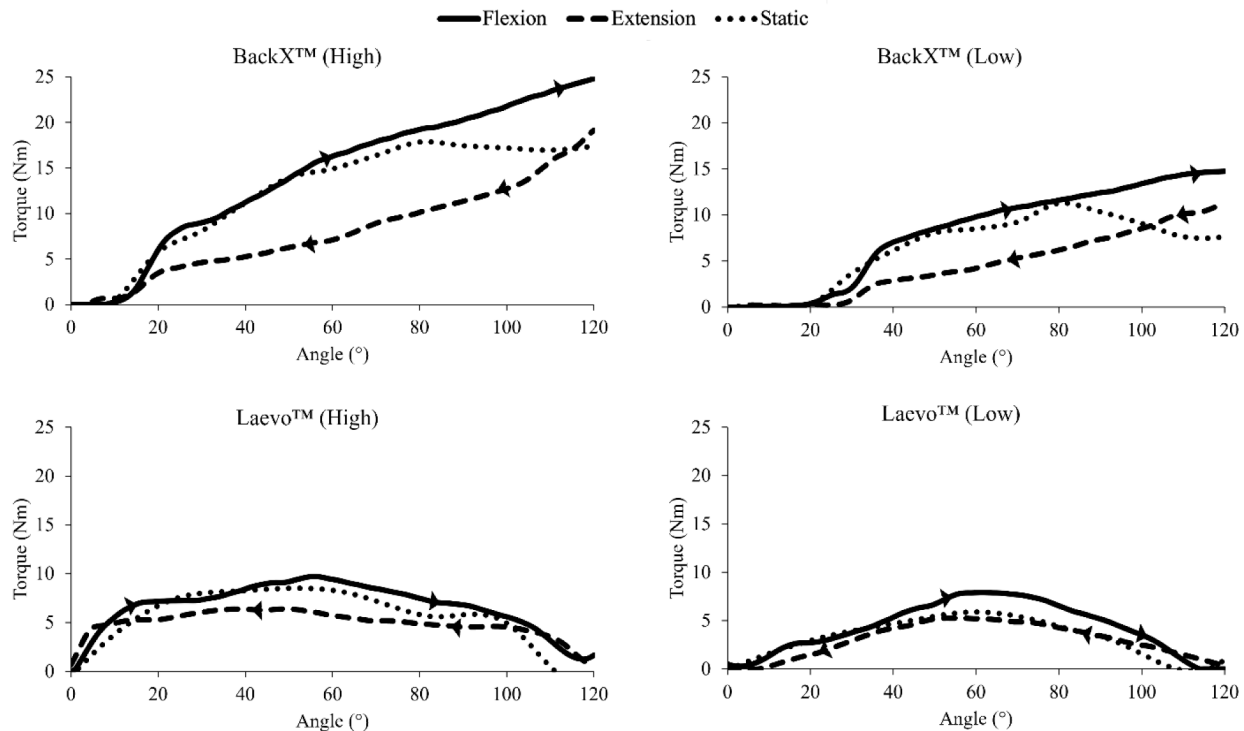


Fig. 2. Demonstration of the experimental setup using human subjects in the trunk modular component (TMC) of the HUMAC NORM. A participant is wearing the BackX™, and the trunk is positioned or moved using the trunk adapter of the dynamometer.





**Fig. 3.** Net torque profiles obtained from the mannequin with the BackX™ and Laevo™ during flexion, extension, and static phases, separated by support settings (High and Low). Net torque profiles are for each (unilateral) mechanism, with dynamic data shown for the 20°/sec condition, and angles indicate hip flexion.

(high and low) in both static and dynamic conditions. With this approach, we obtained raw torque profiles by manipulating hip flexion/extension angles of a mannequin, and trunk flexion/extension angles of a human subject. For both inanimate and animate subjects, comparable ranges of assistive torques were obtained, yet values differed by up to ~10 Nm depending on the joint angle (Fig. 5). The use of the human subjects also produced effective torque profiles only over a relatively narrower range of joint angles due to several practical limitations as discussed below.

Our results indicate that in case passive BSEs are used for heavy lifting tasks, they may provide higher hip/trunk extension torque during the lowering (i.e., trunk flexion) phase than the lifting (i.e., trunk extension) phase. Given that lumbar mechanical loads can be higher during lifting vs lowering – including external flexion moments (Lee & Nussbaum, 2012) and lumbar extensor muscle activation (Madinei et al., 2020) – the lower level of support provided in this phase may suggest that the design is suboptimal. Furthermore, the higher hip/trunk extension torque provided by the BSE during the lowering phase could increase chest discomfort if the device has a chest pad coupled with torque generators (as was the case for the BSEs used in this study). Active exoskeletons, with controllable torque profiles, could address these limitations of passive BSEs.

In the dynamic condition (i.e., flexion/extension speed > 0°/sec.), larger assistive torques were generated during the flexion vs extension phases (Fig. 3), consistent with the finding of Koopman et al. (2020; 2019). They also reported no effect of flexion/extension speed on torque profiles and noted that the difference between torques during the flexion and extension phases is due to friction in the torque generation mechanism. We similarly found no obvious effect of controlled flexion/extension speeds (Fig. A1). Both the BackX™ and Laevo™ utilize a gas-spring mechanism for torque generation (Kazerooni et al., 2019; Panero et al., 2021). As is typical of a gas spring, friction forces are added or subtracted to static forces generated respectively when being compressed (i.e., flexion phase) or extended (i.e., extension phase). The BackX™ (vs Laevo™) had a larger difference in assistive torques

between the flexion and extension phases, indicating that friction forces in the torque generation mechanism may be higher for this device (Fig. 3). While the use of gas springs might be anticipated to yield velocity-dependent effects, it is possible that such effects are only observable outside the kinematic range tested here. Interestingly, some assistive torques were generated even when the torque-generating mechanism was not engaged (i.e., BSE<sub>OFF</sub>), with peak values on the order of 5–10 Nm. These torques were higher for the Laevo™ vs BackX™ (Fig. A2), and likely were caused by intrinsic resistance/friction present in the torque generation mechanism.

Assistive torque profiles in the static condition obtained for Laevo™ here were comparable with the results reported by Koopman et al. (2019). Specifically, the Laevo™ was estimated here to generate total net torques (i.e., combined bilateral mechanisms) of up to ~18 Nm depending on the support setting. Similarly, the torques reported by Koopman et al. (2019) were mainly lower than 20 Nm at different bending angles (see Fig. 4 in their paper). Results for the dynamic condition found here were also comparable to those reported by Koopman et al. (2020), though only when aggregating the raw torque profiles from the BSE<sub>OFF</sub> and BSE<sub>ON</sub> conditions. Specifically, the Laevo™ was estimated here to generate total net torques (i.e., combined bilateral mechanisms) of up to ~40 Nm depending on the support setting and bending direction, and Koopman et al. (2020) reported similar torques within the same range of motion. Further, the net torque profile pattern found here for the Laevo™ (i.e., inverse parabolic shape with maximum torque at ~50–60°) was comparable to those of Koopman et al. (2020). This combined effect of BSE<sub>OFF</sub> and BSE<sub>ON</sub> conditions is further evident from Fig. A2, which shows a similar pattern and torque magnitude compared to those of Koopman et al. (2020); note, though, that the net torques presented here need to be multiplied by two for direct comparison. We believe the raw torques obtained from the BSE<sub>OFF</sub> condition incorporate the effects from the mechanical properties of the BSEs (e.g., mass, moment of inertia, strap tension, intrinsic stiffness of the torque generation mechanism), and such effects were extracted from the torque measurements. Future research, however, is needed to develop a unified

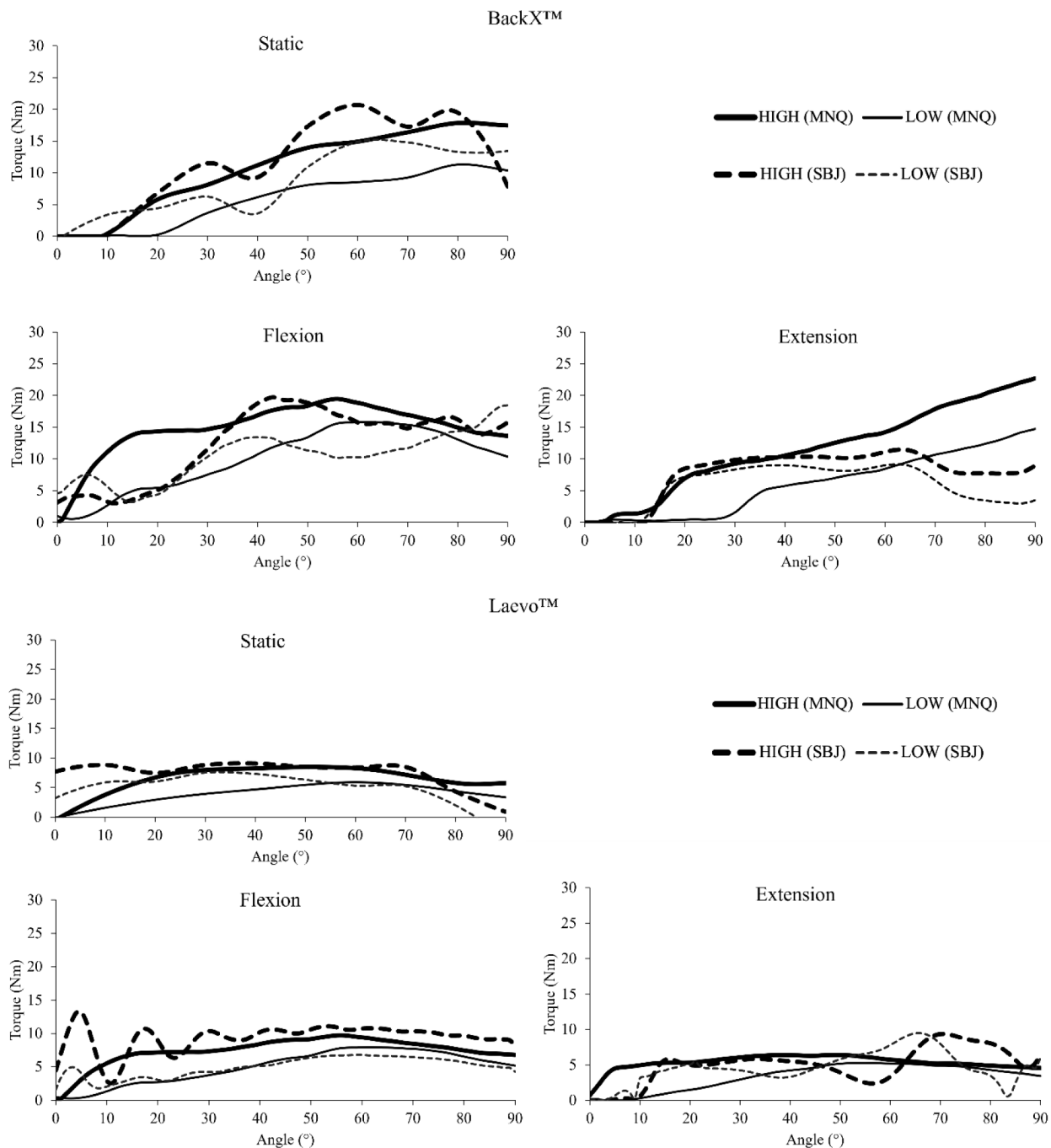


**Fig. 4.** Net torque profiles obtained from the mannequin (MNQ) and human subjects (SBJ) for BackX<sup>TM</sup> (top) and Laevo<sup>TM</sup> (bottom) in two support conditions (LOW and HIGH), separated by static and dynamic (i.e., flexion and extension phases) conditions. Torque profiles are for each (unilateral) mechanism, with dynamic data shown for the 20°/sec condition.

approach to measuring and presenting the assistive torques of exoskeletons.

As noted above, we also measured the raw torque profiles generated by the mannequin without “wearing” the BSEs (i.e., NO BSE) to determine any offset torques caused by the mannequin and the dynamometer adapter (e.g., mass, moment of inertia, intrinsic stiffness in the mannequin “thigh” joint). These raw torque profiles are presented in Fig. A3. The NO BSE condition was estimated to generate flexion/extension raw torques of up to ~8 Nm during both static and dynamic conditions. These torque values are within similar ranges measured for the BSE<sub>OFF</sub> condition, though only for the BackX<sup>TM</sup>. This inconsistency between the NO BSE and BSE<sub>OFF</sub> Laevo<sup>TM</sup> torque profiles might stem from the

intrinsic stiffness (or resistance) present in the Laevo<sup>TM</sup> torque generation mechanism, whereas BackX<sup>TM</sup> appears to have a low intrinsic stiffness (or resistance) in the BSE<sub>OFF</sub> condition. These findings thus indicate that exoskeleton-generated torque profiles might differ depending on the method used for defining the assistive torque of a BSE. Future research is clearly needed to better understand the contribution of the intrinsic stiffnesses/resistance of the BSE torque generation mechanisms to the actual torque that users experience.

Measuring supportive torque profiles while a human subject wears a BSE may provide more realistic torque profiles, such as by capturing relative motions between the BSE and the human user. With the current approach, though, we found it challenging to measure torque profiles

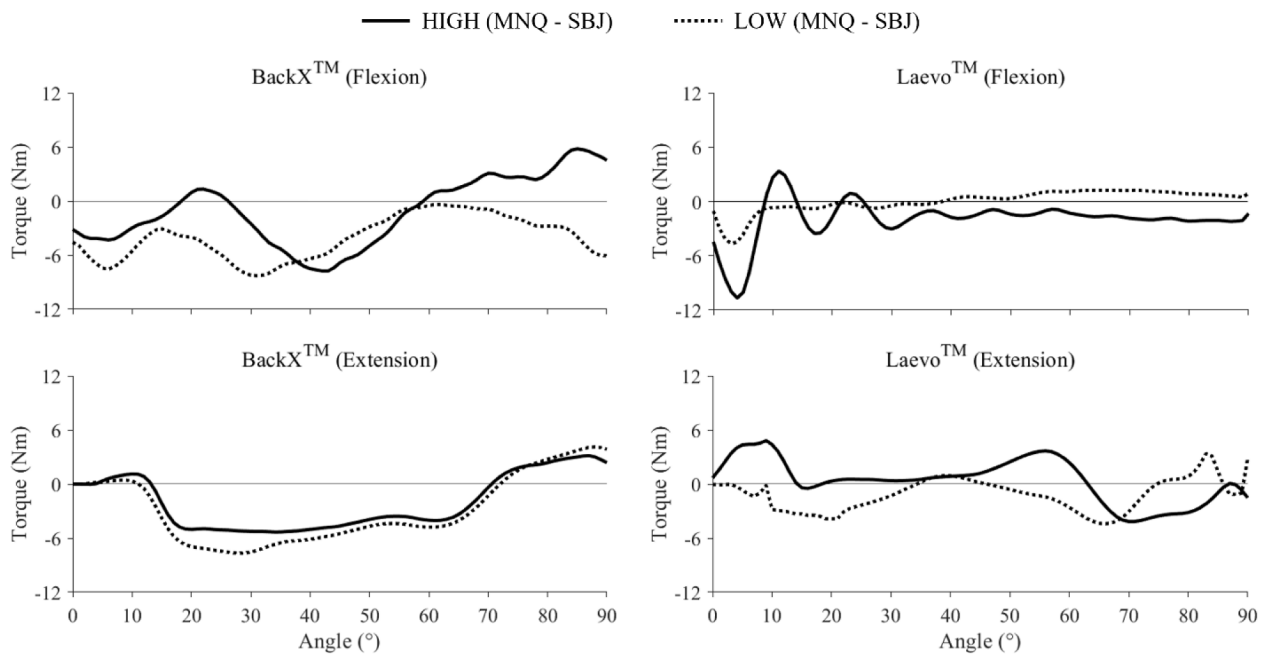


**Fig. 5.** Differences in mean net torque profiles obtained from the mannequin (MNQ) and human subjects (SBJ). Results are shown for the two exoskeletons in both flexion and extension as a function of hip joint angle.

using human subjects, especially during dynamic conditions. BSE torque profiles obtained using human subjects were often within a similar range as those obtained using the mannequin, yet they were also not always consistent (Fig. 5). Torque profiles in the static condition were more comparable than in the dynamic condition over a larger range of flexion/extension angles examined. Differences in torques on the order of 0–10 Nm were evident (Fig. 5), and these differences were non-trivial in some cases. Given that peak RA muscle activity was rather small, suggesting minimal active torque generation, we posit that the noted challenges in measuring assistive torques using human subjects under a dynamic condition arise from some combination of several sources:

- When accelerating to reach a target flexion/extension angular velocity, or decelerating to stop, rotational moments due to the inertia of a participant's trunk and the dynamometer trunk adapter occur in a direction opposite to movement. This effect results mainly because the continuous passive mode of the dynamometer was used, so that the trunk of a participant was moved passively by the dynamometer, rather than the participant voluntarily flexing/extending the trunk. In addition, effects of wobbling masses in the human trunk can affect measured torques during angular acceleration and deceleration (e.g., Bazrgari et al., 2011). A more gradual angular acceleration/deceleration could help, though would still limit the angular range over which isokinetic data could be obtained.
- There is a limit on the feasible trunk range-of-motion using the TMC of the dynamometer when a participant is inside and wearing a BSE. Participants reported considerable discomfort beyond 90° of trunk flexion while in the TMC. Of note, the supine position used for the mannequin allowed a large range-of-motion (0–120°). Yet, our preliminary testing indicated that position still presented difficulties with human subjects, such as discomfort with hip flexed exceeded 90–100° and lack of control over knee movements.
- A possible misalignment of the hip flexion axis and the axis of rotation for the dynamometer adapter could have resulted in a mismatch between human subject results and the mannequin results, despite tightly securing the subjects to the trunk adapter of the dynamometer.

In summary, we captured net torque profiles of BSEs using a

computerized dynamometer in both static and dynamic conditions and with different BSE support settings. This approach permits control over joint kinematics and appears to be more effective using a mannequin vs human subjects. Future work is recommended to assess this approach for other occupational exoskeletons, such as soft devices (exosuits) and for arm-support exoskeletons. Characterizing exoskeleton assistive torque profiles can help in better understanding how to select a torque profile for given task requirements and user anthropometry, and assist in predicting the potential impacts of exoskeleton use by incorporating measured torque profiles in a musculoskeletal modeling system.

#### CRediT authorship contribution statement

**Saman Madinei:** Writing – review & editing, Writing – original draft, Project administration, Methodology, Investigation, Formal analysis, Conceptualization. **Sunwook Kim:** Writing – review & editing, Writing – original draft, Supervision, Methodology, Conceptualization. **Jang-Ho Park:** Writing – review & editing, Writing – original draft, Methodology, Investigation, Conceptualization. **Divya Srinivasan:** Writing – review & editing, Writing – original draft, Supervision, Methodology, Conceptualization. **Maury A. Nussbaum:** Writing – review & editing, Writing – original draft, Supervision, Project administration, Methodology, Investigation, Conceptualization.

#### Declaration of Competing Interest

The authors declare that they have no known competing financial interests or personal relationships that could have appeared to influence the work reported in this paper.

#### Acknowledgment

All authors have made substantial contributions to all of the following: (1) the conception and design of the study, or acquisition of data, or analysis and interpretation of data, (2) drafting the article or revising it critically for important intellectual content, (3) final approval of the version to be submitted.

## Appendix A. Supplementary material

Supplementary data to this article can be found online at <https://doi.org/10.1016/j.jbiomech.2022.111363>.

## References

- Agarwal, P., Neptune, R.R., Deshpande, A.D., 2016. A simulation framework for virtual prototyping of robotic exoskeletons. *J. Biomech. Eng.* 138 (6).
- Alabdulkarim, S., Nussbaum, M.A., 2019. Influences of different exoskeleton designs and tool mass on physical demands and performance in a simulated overhead drilling task. *Appl. Ergon.* 74, 55–66.
- Alemi, M.M., Madinei, S., Kim, S., Srinivasan, D., Nussbaum, M.A., 2020. Effects of two passive back-support exoskeletons on muscle activity, energy expenditure, and subjective assessments during repetitive lifting. *Hum. Factors* 62 (3), 458–474.
- Baltrusch, S.J., van Dieën, J.H., Bruijn, S.M., Koopman, A.S., van Bennekom, C.A.M., Houdijk, H., 2019. The effect of a passive trunk exoskeleton on metabolic costs during lifting and walking. *Ergonomics* 62 (7), 903–916.
- Bartel, D.L., Davy, D.T., 2006. *Orthopaedic biomechanics: mechanics and design in musculoskeletal systems*. Prentice Hall.
- Bazrgari, B., Nussbaum, M., Madigan, M., Shirazi-Adl, A., 2011. Soft tissue wobbling affects trunk dynamic response in sudden perturbations. *J. Biomech.* 44 (3), 547–551.
- Criswell, E., 2010. *Cram's introduction to surface electromyography*. Jones & Bartlett Publishers.
- de Kruif, B.J., Schmidhauser, E., Stadler, K.S., O'Sullivan, L.W., 2017. Simulation architecture for modelling interaction between user and elbow-articulated exoskeleton. *J. Bionic Eng.* 14 (4), 706–715.
- Ferreira, G., Gaspar, J., Fújão, C., Nunes, I.L., 2020. *Piloting the Use of an Upper Limb Passive Exoskeleton in Automotive Industry: Assessing User Acceptance and Intention of Use*. Paper presented at the International Conference on Applied Human Factors and Ergonomics.
- Fritzsche, L., Gärtner, C., Spitzhörn, M., Galibarov, P. E., Damsgaard, M., Maurice, P., Babić, J., 2021. *Assessing the Efficiency of Industrial Exoskeletons with Biomechanical Modelling—Comparison of Experimental and Simulation Results*. Paper presented at the Congress of the International Ergonomics Association.
- Hensel, R., Keil, M., 2019. Subjective evaluation of a passive industrial exoskeleton for lower-back support: A field study in the automotive sector. *IIEE Trans. Occup. Ergon. Human Factors* 7 (3–4), 213–221.
- Hyun, D.J., Bae, K., Kim, K., Nam, S., Lee, D.-H., 2019. A light-weight passive upper arm assistive exoskeleton based on multi-linkage spring-energy dissipation mechanism for overhead tasks. *Rob. Auton. Syst.* 122, 103309.
- Jensen, E.F., Raunsbæk, J., Lund, J.N., Rahman, T., Rasmussen, J., Castro, M.N., 2018. Development and simulation of a passive upper extremity orthosis for amyoplasia. *J. Rehab. Assistive Technol. Eng.*, 5, 2055668318761525.
- Kazerooni, H., Tung, W., Pillai, M., 2019. *Evaluation of trunk-supporting exoskeleton*. Paper presented at the Proceedings of the Human Factors and Ergonomics Society Annual Meeting.
- Khamar, M., Edrisi, M., Zahiri, M., 2019. Human-exoskeleton control simulation, kinetic and kinematic modeling and parameters extraction. *MethodsX* 6, 1838–1846.
- Kim, S., Nussbaum, M.A., Esfahani, M.I.M., Alemi, M.M., Alabdulkarim, S., Rashedi, E., 2018. Assessing the influence of a passive, upper extremity exoskeletal vest for tasks requiring arm elevation: Part I—“Expected” effects on discomfort, shoulder muscle activity, and work task performance. *Appl. Ergon.* 70, 315–322.
- Kim, S., Moore, A., Srinivasan, D., Akanmu, A., Barr, A., Harris-Adamson, C., Rempel, D. M., Nussbaum, M.A., 2019. Potential of exoskeleton technologies to enhance safety, health, and performance in construction: Industry perspectives and future research directions. *IIEE Trans. Occup. Ergon. Human Factors* 7 (3–4), 185–191.
- Kim, S., Nussbaum, M.A., Smets, M., Ranganathan, S., 2021. Effects of an arm-support exoskeleton on perceived work intensity and musculoskeletal discomfort: An 18-month field study in automotive assembly. *Am. J. Ind. Med.* 64 (11), 905–914.
- Koopman, A.S., Kingma, I., Faber, G.S., de Looze, M.P., van Dieën, J.H., 2019. Effects of a passive exoskeleton on the mechanical loading of the low back in static holding tasks. *J. Biomech.* 83, 97–103.
- Koopman, A.S., Kingma, I., de Looze, M.P., van Dieën, J.H., 2020. Effects of a passive back exoskeleton on the mechanical loading of the low-back during symmetric lifting. *J. Biomech.* 102, 109486.
- Lavender, S.A., Marras, W.S., Ferguson, S.A., Splittstoesser, R.E., Yang, G., 2012. Developing physical exposure-based back injury risk models applicable to manual handling jobs in distribution centers. *J. Occup. Environ. Hygiene* 9 (7), 450–459.
- Lee, J., Nussbaum, M.A., 2012. Experienced workers exhibit distinct torso kinematics/kinetics and patterns of task dependency during repetitive lifts and lowers. *Ergonomics* 55 (12), 1535–1547.
- Madinei, S., Alemi, M.M., Kim, S., Srinivasan, D., Nussbaum, M.A., 2020. Biomechanical assessment of two back-support exoskeletons in symmetric and asymmetric repetitive lifting with moderate postural demands. *Appl. Ergon.* 88, 103156 <https://doi.org/10.1016/j.apergo.2020.103156>.
- Marras, W.S., Lavender, S.A., Leurgans, S.E., Rajulu, S.L., Allread, S.W.G., Fathallah, F. A., Ferguson, S.A., 1993. The role of dynamic three-dimensional trunk motion in occupationally-related. *Spine* 18 (5), 617–628.
- Marras, W.S., Mirka, G.A., 1993. Electromyographic studies of the lumbar trunk musculature during the generation of low-level trunk acceleration. *J. Orthop. Res.* 11 (6), 811–817. <https://doi.org/10.1002/jor.1100110606>.
- Moore, A., Kim, S., Srinivasan, D., Nussbaum, M.A., Ojelade, A., Harris-Adamson, C., Gutierrez Contreras, N., Barr, A., Rempel, D., 2021. A preliminary decision tree modeling of factors that determine readiness to use exoskeletons in construction. *Proceedings of the Human Factors and Ergonomics Society Annual Meeting* 65 (1), 419–420. <https://doi.org/10.1177/1071181321651014>.
- Nussbaum, M.A., Lowe, B.D., de Looze, M., Harris-Adamson, C., Smets, M., 2019. An introduction to the special issue on occupational exoskeletons. Taylor & Francis.
- Panero, E., Segagliari, M., Pastorelli, S., Gastaldi, L., 2021. *Kinematic and Dynamic Assessment of Trunk Exoskeleton*, Cham.
- Thamsuwan, O., Milosavljevic, S., Srinivasan, D., Trask, C., 2020. Potential exoskeleton uses for reducing low back muscular activity during farm tasks. *Am. J. Ind. Med.* 63 (11), 1017–1028.
- Upasani, S., Franco, R., Niewolny, K., Srinivasan, D., 2019. The potential for exoskeletons to improve health and safety in agriculture—Perspectives from service providers. *IIEE Trans. Occup. Ergon. Human Factors* 7 (3–4), 222–229.
- Zhou, X., Chen, X., 2021. Design and Evaluation of Torque Compensation Controllers for a Lower Extremity Exoskeleton. *J. Biomech. Eng.* 143 (1), 011007.